ISSN: 2687-8097
Scientific Journal of Research and Reviews
DOI: 10.33552/SJRR.2026.05.000605
Iris Publishers

Research Article

A Hybrid BiLSTM-GRU-PINN Deep Learning Framework for Modeling Regional Climate and Extreme Weather Forecasting in the Semi-Arid of Ghana

Toufic Seini[1]*, Oluwole Daniel Makinde[2] and Ibrahim Yakubu Seini[1]

[1]*Department of Mathematics, Faculty of Physical Sciences, University for Development Studies, Ghana*

[2]*Faculty of Military Science, Stellenbosch University, South Africa*

***Corresponding author:** Toufic Seini, Department of Mathematics, Faculty of Physical Sciences, University for Development Studies, P.O. Box, TL 1350, Tamale, 233, Northern Region, Ghana.

Received Date: August 19, 2026

Published Date: August 31, 2026

Abstract

Accurate climate and weather forecasting remains a critical challenge in semi-arid regions like northern Ghana, where climate variability increasingly threatens agriculture, water security, and rural livelihoods. This study proposes a novel hybrid deep learning framework, BiLSTM-GRU-PINN, that combines Bidirectional Long Short-Term Memory (BiLSTM), Gated Recurrent Units (GRU), and Physics-Informed Neural Networks (PINNs) for enhanced regional climate prediction. The framework integrates the temporal modeling capabilities of BiLSTM and GRU with the physical consistency of PINNs, incorporating partial differential equations such as the heat equation directly into the model's loss function. The system is trained on multi-source historical and observational data, including records from GMet, CMIP6, and NASA EarthData, and is evaluated using metrics such as RMSE, MAE, and prediction accuracy. The rresults demonstrate that the BiLSTM-GRU-PINN model significantly outperforms conventional models, including standalone LSTM, GRU, PINN, and statistical or physics-based approaches in both temperature and rainfall prediction. The best-performing configuration achieved RMSE values of 0.225 for temperature and 0.140 for rainfall, with respective prediction accuracies of 87.78% and 69.76%. Visualization and decomposition analyses show that the model effectively captures long-term trends and seasonal patterns in temperature, while highlighting challenges in predicting the stochastic nature of rainfall. These findings underscore the value of integrating data-driven and physics-based approaches for climate forecasting in data-scarce regions. The proposed framework offers a robust, interpretable, and scalable solution for supporting early warning systems, policy-making, and climate adaptation strategies across semi-arid and similarly vulnerable contexts in Africa..

Keywords: BiLSTM-GRU-PINN, Hybrid Deep Learning, Physics-Informed Neural Networks, Climate Forecasting, Rainfall Prediction, Temperature Prediction, Stochastic Differential Equations, Partial Differential Equations, Semi-Arid Ghana

Introduction

Climate variability and extreme weather events pose significant challenges to ecosystems and human livelihoods, particularly in semi-arid regions where socioeconomic activities such as agriculture, water management, and public health are highly sensitive to climatic conditions [1,2]. In northern Ghana, increasing unpredictability in rainfall patterns and rising temperatures have exacerbated the frequency and intensity of droughts and flash floods, threatening food security and rural resilience [3,4]. Accurate and timely regional climate forecasting is therefore critical for early warning systems, adaptive planning, and sustainable development in this vulnerable region.

Traditional climate modeling approaches rely heavily on numerical simulations based on partial differential equations (PDEs), such as the Navier-Stokes and heat equations, which describe the physical dynamics of the atmosphere with strong theoretical foundations [5,6]. While these physics-based models offer interpretability and consistency with natural laws, they are often computationally intensive, require high-resolution input data, and struggle to capture localized, nonlinear phenomena, particularly in data-scarce regions like semi-arid Ghana [7,8]. Moreover, global and regional climate models (GCMs/RCMs) frequently lack the spatial and temporal resolution needed for actionable, community-level predictions. To address these challenges, data-driven approaches, particularly machine learning (ML), should be integrated because of their ability to extract complex, non-linear patterns from large and heterogeneous climate datasets [9-11]. ML models offer a flexible and efficient alternative, capable of capturing temporal and spatial dependencies without explicit programming of physical laws. Recent advances have further demonstrated the value of integrating ML with domain knowledge, as seen in hybrid modeling frameworks that combine data-driven learning with physical constraints [12].

In recent years, machine learning (ML) has emerged as a powerful data-driven alternative capable of identifying complex patterns in large-scale climatic datasets. Techniques such as Long Short-Term Memory (LSTM) and Gated Recurrent Units (GRU) have demonstrated success in modeling time-series data, including rainfall and temperature forecasting [13,14]. However, purely data-driven models often function as black boxes, lacking physical consistency and generalizability, especially when training data are limited or noisy.

To bridge this gap, this study proposes a hybrid deep learning framework that integrates the strengths of data-driven machine learning with the physical fidelity of differential equation models. Specifically, the research introduces a novel BiLSTM-GRU-PINN architecture combining Bidirectional LSTM (BiLSTM), GRU, and Physics-Informed Neural Networks (PINNs) to enhance regional climate and extreme weather forecasting in semi-arid Ghana. The BiLSTM layer captures long-term temporal dependencies in both forward and backward directions, while the GRU layer compresses sequential information efficiently. Crucially, the PINN component incorporates physical laws such as the heat equation into the loss function, ensuring that the model predictions remain consistent with atmospheric dynamics even in data-limited settings [15]. The primary objective of this study is to develop and validate a hybrid modeling framework that improves the accuracy, efficiency, and physical interpretability of climate predictions in northern Ghana. By fusing data-driven learning with physical constraints, this research aims to deliver a robust, interpretable, and scalable forecasting tool that supports climate adaptation, disaster preparedness, and policy-making in vulnerable semi-arid regions not only in Ghana but across similar agro-climatic zones in Africa and beyond.

Despite the critical need for accurate regional climate forecasting in semi-arid Ghana, existing modeling approaches face significant limitations. Global climate models (GCMs) often lack sufficient spatial resolution to capture localized climatic variations, while regional models frequently fail to adequately represent complex local atmospheric dynamics and land-atmosphere interactions. Furthermore, many current frameworks do not fully integrate observational and historical climate data, leading to reduced predictive accuracy. Deterministic models, although grounded in physical laws, struggle to capture the inherent non-linearities associated with extreme weather events such as droughts and flash floods [16]. These challenges underscore the need for a hybrid modeling framework that synergistically combines data-driven machine learning techniques with physics-based differential equation models to enhance the accuracy, reliability, and regional specificity of climate and extreme weather predictions.

Figure 1 shows the study area of diverse climate zones with the risk of drought as a result of high temperatures and low rainfall, especially in the northern part of Ghana.

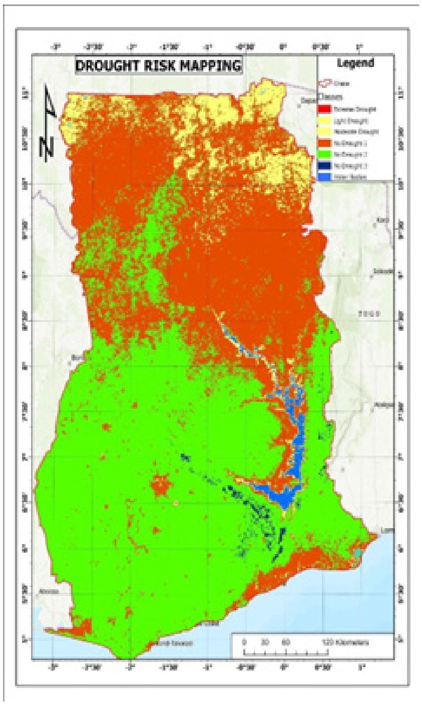

Figure 1: Ghana map showing the diverse climate, including the semi-arid zone [45].

This study is motivated by the need to develop a robust, interpretable, and scalable framework that integrates the strengths of both paradigms, machine learning and physics-based modeling. This integrated approach addresses critical gaps in current modeling frameworks and is especially suited to data-sparse regions where observational datasets are limited. The model's ability to learn complex temporal patterns while respecting the governing physics makes it a compelling tool for climate resilience planning and early warning systems in Ghana and similar regions across Sub-Saharan Africa.

Accurate prediction of regional climate and extreme weather events in semi-arid regions such as Northern Ghana remains a formidable scientific challenge. These regions are characterized by complex interactions between large-scale atmospheric dynamics and localized bio geophysical processes, including soil moisture variability, land cover changes, and surface energy fluxes. The increasing frequency and intensity of climate extremes such as droughts and flash floods have profound implications for agriculture, water security, public health, and rural livelihoods [17,18]. In Northern Ghana, rising climate variability has disrupted traditional farming cycles and exacerbated water scarcity, underscoring the urgent need for reliable, high-resolution forecasting systems [3].

Historically, climate modeling has relied on physics-based numerical models governed by systems of differential equations that describe the conservation of mass, momentum, and energy in the atmosphere. These models, including General Circulation Models (GCMs) and Regional Climate Models (RCMs), simulate climatic processes with strong theoretical foundations [6]. RCMs, in particular, enhance spatial resolution by dynamically downscaling GCM outputs using partial differential equations (PDEs) such as the Navier-Stokes equations, shallow water equations, and heat diffusion models. Although these models provide physically consistent representations of atmospheric behavior, they face significant limitations in semi-arid regions like Ghana. These include high computational demands, sensitivity to initial and boundary conditions, and difficulties in accurately representing sub-grid-scale processes such as convection and land-atmosphere feedbacks [5,7]. To overcome these limitations, ML models remain the ultimate best in extracting complex spatiotemporal patterns from large-scale climate datasets without explicit programming of physical laws. Also, techniques like Long Short-Term Memory (LSTM) networks, Gated Recurrent Units (GRUs), and Convolutional Neural Networks (CNNs) have demonstrated strong performance in rainfall and temperature prediction [13,14]. LSTM models have been successfully applied to rainfall forecasting in West Africa, where they outperformed traditional statistical models in capturing non-linear temporal dependencies [19]. Similarly, GRU-based models have shown efficiency in handling long sequences with reduced computational overhead, making them suitable for real-time forecasting applications [20].

One of the most critical shortcomings of traditional models is their limited ability to capture the non-linear and chaotic nature of extreme weather events. For instance, heavy rainfall episodes and prolonged dry spells often emerge from complex, non-linear interactions that are poorly resolved by deterministic solvers, leading to underestimation of risk and reduced forecast skill [21]. Additionally, the scarcity and inconsistency of observational data in many African regions further compromise model calibration and validation, increasing uncertainty in projections [4].

In response to these challenges, machine learning (ML) has emerged as a powerful complementary tool in climate science. Unlike physics-based models, ML algorithms excel at identifying complex, non-linear patterns in large, high-dimensional datasets without requiring explicit formulation of governing equations. Techniques such as deep neural networks, ensemble methods, and time-series models have demonstrated strong performance in various hydrometeorological applications. For example, Long Short-Term Memory (LSTM) and Gated Recurrent Unit (GRU) networks have been successfully applied to rainfall forecasting and temperature forecasting due to their ability to model long-term temporal dependencies [13]. Similarly, tree-based models like Random Forest and XGBoost have been used for drought prediction and climate classification with high accuracy [23]. Moreover, ML-based downscaling methods, such as DeepSD [24], have enabled the generation of high-resolution climate projections from coarse GCM outputs, enhancing regional applicability.

Despite their predictive power, purely data-driven models are often criticized as "black boxes" due to their lack of physical interpretability and potential for overfitting, especially in data-scarce environments. Their performance may degrade when extrapolating beyond the range of training data, limiting their reliability for long-term climate projections [25,26]. This has led to growing interest in hybrid modeling frameworks that integrate the strengths of both physics-based and data-driven approaches. This groundbreaking advancement in the domain of Physics-Informed Neural Network (PINN) framework was introduced by [15]. PINNs embed governing PDEs directly into the loss function of a neural network, ensuring that predictions remain consistent with physical laws such as conservation of mass and energy. This approach enhances model robustness, especially in data-scarce environments, and reduces overfitting by constraining the solution space [27,28], and improves performance in low-data regime conditions commonly encountered in sub-Saharan Africa. PINNs have been successfully applied to fluid dynamics, heat transfer, and subsurface flow modeling, demonstrating their potential in geophysical applications [29,30]. Other hybrid strategies include using ML for bias correction of numerical model outputs, data assimilation, and parameterization of sub-grid processes [31,32]. These methods allow for dynamic updating of model states using real-time observations, thereby improving forecast accuracy and adaptability.

In the context of climate modeling, hybrid frameworks like BiLSTM-GRU-PINN represent a novel integration strategy [33]. The bidirectional LSTM (BiLSTM) layer captures temporal dependencies in both forward and backward directions, enabling the model to learn from past and future context within a sequence. The GRU layer then compresses this information efficiently, reducing redundancy and computational load. Finally, the PINN component regularizes the model by incorporating physical constraints, such as the heat equation for temperature diffusion into the training process. This ensures that even when observational data are limited or noisy, the model remains physically plausible. Some recent studies have begun to explore the application of such hybrid models in African contexts. In the work of [34] developed a physics-informed

LSTM model to predict drought onset in Ghana, showing improved accuracy over standalone ML models. Similarly, [35] applied a hybrid CNN-PINN framework to downscale rainfall projections in Nigeria, achieving higher spatial resolution and better alignment with observed patterns. These studies underscore the growing interest in merging data-driven and physics-based approaches to improve climate services in West Africa.

In the case of extreme weather prediction, hybrid ML enhanced models have shown promise in augmenting traditional climate modeling by learning complex patterns from data without requiring explicit physical laws [36]. Convolutional neural networks (CNN) have been used to forecast tropical cyclone intensities by analyzing satellite imagery [37], while Random Forest models have enabled short-term forecasting of flash floods in data-sparse regions [38]. Generative Adversarial Networks (GANs) have also been employed to super-resolve coarse climate model outputs, generating high-resolution rainfall fields that better represent localized convection [39]. In Ghana, extreme events are often driven by mesoscale convective systems and land-surface feedbacks that are inadequately captured by global models [40]. Integrating satellite-derived datasets, such as CHIRPS rainfall estimates and MODIS land surface temperature, into ML frameworks offers a viable pathway to improve early warning systems [41].

Despite these advances, the application of hybrid ML-PDE models in West Africa, and Ghana in particular, remains limited. Existing studies in the region have primarily relied on standalone RCMs or statistical models. For instance, [14] applied ML models to predict rainfall in Burkina Faso with notable accuracy and [4] utilized the SWAT hydrological model to assess climate change impacts on the Volta Basin, while [42,43] employed regression-based techniques to project future rainfall and temperature trends. However, these approaches rarely incorporate machine learning, and even more rarely integrate physical laws into data-driven models. Furthermore, climate model outputs are often not translated into actionable insights for policymakers, limiting their utility in agriculture planning, disaster preparedness, and climate adaptation strategies [22, 44].

The integration of machine learning with differential equation-based models represents a transformative opportunity for climate science in vulnerable, data-scarce regions. Although both methodologies have been explored independently, their synergistic application, particularly in the form of hybrid architectures such as BiLSTM-GRU-PINN, remains underexplored in the African context, especially in Ghana. This research addresses this critical gap by developing a novel, physics-informed deep learning framework tailored to the unique climatic and socio-environmental conditions of semi-arid Ghana. By combining the pattern recognition power of deep learning with the physical consistency of PDEs, the proposed model aims to deliver accurate, interpretable, and policy-relevant climate and extreme weather forecasts.

Table 1 and Table 2 compares the proposed BiLSTM-GRU-PINN model with other prominent climate and weather forecasting models, including their model type, methodology, strengths, limitations, and application context.

Table 1: Overview of climate and weather forecasting models.

Model	Model Type	Core Methodology
BiLSTM–GRU–PINN (Proposed)	Hybrid (Data + Physics)	BiLSTM captures bidirectional temporal dependencies, GRU improves efficiency, and PINN enforces physical laws via heat and rainfall PDEs.
PINNs [15, 27,29]	Physics-guided DL	Governing PDEs are embedded into neural network loss functions to constrain predictions.
LSTM / GRU [19,20]	Data-driven DL	Recurrent neural networks designed for temporal sequence learning.
CNN–PINN [35]	Hybrid (Spatial ML + Physics)	CNN-based spatial feature extraction combined with physics-based regularization.
GCMs / RCMs [6,7]	Physics-based Numerical	Numerical solution of atmospheric PDEs on spatial grids.
SWAT [4,40]	Hydrological Model	Process-based simulation of watershed hydrology and land–climate interactions.
SDE Models [1,3]	Stochastic Models	Rainfall modeled as stochastic differential equations.
PI–LSTM [34]	Hybrid (Temporal ML + Physics)	LSTM regularized using PDE-based constraints.
Adversarial PINNs [27]	Advanced PINN	Adversarial learning used to quantify prediction uncertainty.
DeepXDE [30]	PINN Framework	Open-source toolkit for solving forward and inverse PDEs with PINNs.

Table 2: Strengths and limitations of climate and weather forecasting models.

Model	Key Strengths	Main Limitations
BiLSTM–GRU–PINN (Proposed)	Physical consistency, robustness under noisy data, long-term dependency modeling, improved interpretability.	High computational cost; requires ML and PDE expertise.
PINNs	Physically plausible predictions; effective in low-data regimes; reduced overfitting.	Slow convergence; limited stochastic modeling ability.
LSTM / GRU	Strong time-series learning; flexible sequence handling.	Lack physical constraints; weak generalization in data-scarce regions.
CNN–PINN	High-resolution spatial modeling; physically consistent outputs.	Computationally intensive; needs dense spatial data.
GCMs / RCMs	Strong theoretical foundation; long-term projections.	Very high computational cost; poor local resolution.

SWAT	Well validated; integrates land use and climate.	Extensive calibration; unsuitable for real-time forecasting.
SDE Models	Captures randomness; simple and interpretable.	Univariate focus; stationarity assumption.
PI–LSTM	Balances data and physics; improved accuracy over LSTM.	Limited deployment; still evolving.
Adversarial PINNs	Uncertainty quantification; improved robustness.	Complex architecture; large data requirements.
DeepXDE	Flexible, extensible; supports inverse problems.	Not a standalone predictive model; requires customization.

Methodology

Data Collection and Preprocessing

To achieve the research objectives, comprehensive climate data collection was carried out at the Ghana Meteorological Agency (GMet). Data include climate variables such as rainfall, temperature, soil moisture, and humidity, among others. These serve as the primary input sources for the analysis. The data was further pre-processed to remove noise, gaps, and inconsistencies using Python tools (Pandas, NumPy). Feature selection was performed to identify the most significant variables using Random Forest or Recursive Feature Elimination (RFE) techniques.

Mathematical Modeling

Stochastic Differential Equation Model

To model rainfall dynamics, the stochastic differential equation (SDE) approach will be used, focusing on a mean-reverting Ornstein–Uhlenbeck process. This model is suitable for describing rainfall variability over time and can capture the randomness observed in weather patterns.

The general form of the stochastic differential equation is given by:

$$dR(t)=\theta\left(\mu-R(t)\right)dt+\sigma\,dW(t) \quad (1)$$

Where:

- $R(t)$is the rainfall at time t,
- θ is the rate of mean reversion (describing how fast the rainfall returns to its long-term mean),
- μ is the long-term mean rainfall,
- σ is the volatility (standard deviation),
- W(t) is the Wiener process (Brownian motion) representing the stochastic part of the process.

This equation models the temporal variations in rainfall, allowing us to simulate future precipitation levels based on historical observations.

Seasonal Stochastic Differential Equation (SSDE) for Rainfall

To capture seasonal variations in rainfall dynamics, the study introduce a seasonal term to the SDE model. This extension models periodic fluctuations due to factors like monsoons or dry seasons.

$$dR(t)=\theta\left(\mu-R(t)\right)dt+\sigma\,dW(t)+\alpha\sin(\omega t)\,dt \quad (2)$$

Where:

- α is the seasonal amplitude,
- ω is the frequency of the seasonal cycle (yearly or semi-annual).

Extended SDE Model with External Forcing (Non-Linear Effects)

To account for feedback loops or external factors influencing rainfall, an external forcing term can be added to the SDE model.

$$dR(t)=\theta\left(\mu-R(t)\right)dt+\sigma\,dW(t)+\beta R(t)\,dF(t) \quad (3)$$

Where:

- F(t) is an external forcing function (temperature, ocean circulation),
- β is the coupling factor that determines how strongly R(t) interacts with the forcing term.

Partial Differential Equation Model

For modeling spatial and temporal temperature distribution, partial differential equations (PDEs) will be used. This model will allow us to describe the heat transfer in the atmosphere and other climate variables across different regions, such as temperature changes due to radiation and diffusion in the semi-arid zones.

The general form of the heat equation in the presence of diffusion and source terms is:

$$\frac{\partial T(x,t)}{\partial t}=D\nabla^2 T+Q(x,t)+\phi_{ML}(x,t) \quad (4)$$

Where:

- T(x,t) is the temperature field at location x and time t,
- D is the diffusion coefficient,
- ∇^2 T is the Laplacian operator representing spatial temperature diffusion,
- Q(x,t) is the deterministic heat source term,
- ϕ_{ML} (x,t) represents the correction term derived from machine learning.

The correction term $\phi_{ML}(x,t)$ is added to capture errors and bias arising from conventional modeling, which can be addressed using machine learning techniques.

Heat Equation with Advection (Transport)

To model the transport of heat or other climate variables, an advection term is added to the PDE, representing the movement of heat due to wind or fluid flow.

$$\frac{\partial T(x,t)}{\partial t}=D\nabla^2 T+v\cdot\nabla T+Q(x,t)+\phi_{ML}(x,t) \quad (5)$$

Where:

- v is the velocity vector representing the advection, for instance, wind or fluid flow,
- ∇T is the spatial gradient of temperature.

Nonlinear Diffusion Equation

To account for cases where diffusion is nonlinear, such as near coastlines or mountain ranges, the study introduce a spatially varying diffusion coefficient.

$$\frac{\partial T(x,t)}{\partial t} = D(x,t)\nabla^2 T + Q(x,t) + \phi_{ML}(x,t) \quad (6)$$

Where:

- D(x,t) is a spatially and temporally varying diffusion coefficient that accounts for variable permeability or heat conductivity in the environment.

Nonlinear Source Terms in the Heat Equation

In some cases, the source term Q(x,t) may be nonlinear, depending on factors such as solar radiation, vegetation feedback, or land-surface interactions.

$$\frac{\partial T(x,t)}{\partial t} = D\nabla^2 T + \alpha T^2 + Q(x,t) + \phi_{ML}(x,t) \quad (7)$$

Where:

- αT^2 represents a nonlinear source term that could account for temperature-dependent processes, like radiation feedbacks or biochemical reactions.

Boundary and Initial Conditions for PDEs

To solve the PDE numerically, there is the need appropriate boundary and initial conditions. Common conditions include:

Initial Condition:

$$T(x,0) = T_0(x) \quad (8)$$

Where $T_{0(x)}$ is the initial temperature distribution at time t=0.

Dirichlet Boundary Condition (fixed temperature):

$$T(x_0,t) = T_{boundary} \quad (9)$$

Where x_0 is a boundary point and $T_{boundary}$ is a fixed value.

Neumann Boundary Condition (flux condition):

$$\frac{\partial T(x,t)}{\partial n} = flux \quad (10)$$

Where $\frac{\partial T(x,t)}{\partial n}$ is the derivative of temperature normal to the boundary, representing heat flux.

PINN-Based Loss Functions for SDE and PDE Models

For both the SDE and PDE models, machine learning models can be introduce, such as Physics-Informed Neural Networks (PINNs), to enforce physical laws and improve prediction accuracy.

For the SDE model, the loss function can be:

$$L_{SDE} = \sum \left| \frac{dR(t)}{dt} - \theta(\mu - R(t)) - \sigma dW(t) \right|^2 \quad (11)$$

For the PDE model, the PINN loss function can be:

$$L_{PDE} = \sum \left| \frac{\partial T(x,t)}{dt} - D\nabla^2 T - \alpha T^2 - Q(x,t) \right|^2 \quad (12)$$

Where the model is trained to satisfy these physical equations in addition to learning from observed data, ensuring both physical accuracy and data-driven flexibility.

Experimental Setup

In this experiment, the study aim to predict temperature and rainfall using a deep learning model that combines Bidirectional LSTM (BiLSTM), GRU (Gated Recurrent Units), and Physics-Informed Neural Networks (PINN). The process begins with data preparation, where the dataset is cleaned, and features such as temperature, rainfall, month, and year are normalized using Min Max Scaler. New features like the month and year are also extracted and normalized to provide temporal and seasonal context.

The dataset is split into training (70%), validation (15%), and test (15%) sets. The Time series Generator is used to create sequences of 36 timesteps for training. The model architecture consists of a BiLSTM layer for capturing both forward and backward temporal dependencies, followed by a GRU layer and a dense layer with Re LU activation. The model is regularized using PINN, ensuring predictions respect physical principles like heat diffusion.

During training, the model is compiled with the Adam optimizer and a learning rate of 0.0003. Early stopping is used to prevent overfitting, and the learning rate is reduced if the validation loss plateaus. Hyperparameter tuning is performed to optimize parameters such as the number of units in the BiLSTM-GRU-PINN layers, dropout rate, and learning rate, using grid search or random search to identify the best combination for maximum accuracy.

The model's performance is evaluated on the test set using RMSE, MAE, and prediction accuracy. For forecasting, the trained model predicts the next 12 months of temperature and rainfall, and these predictions are compared with actual historical data rainfall from a Stochastic Differential Equation (SDE), providing a baseline comparison.

BiLSTM-GRU-PINN Model Architecture

The proposed model architecture is presented in Figure 2 below:

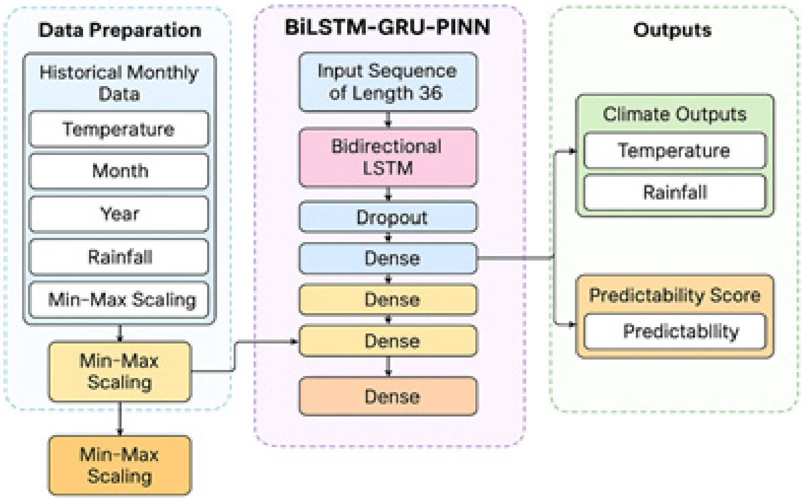

Figure 2: BiLSTM-GRU-PINN model architecture.

Input Representation

A time-series sequence of climate data was considered, where each sample is a multivariate input vector. A sliding window of length L is used for training.

$$X = \left[x_{t-L+1}, x_{t-L+2}, \cdots, x_t\right] \in \mathbb{R}^{L \times d} \qquad (13)$$

Where:

- L=36 is the sequence length (timesteps).
- d=4 is the number of features: Temperature, Rainfall, Month, Year.

Bidirectional LSTM (BiLSTM) Layer

The first layer of the model is a bidirectional LSTM, which captures temporal dependencies in both forward and backward directions. It consists of two LSTM units; one processes the sequence in the forward direction and the other in the backward direction. This allows the model to capture both past and future temporal dependencies, making it more effective in time-series forecasting tasks. By combining both outputs, the study gain richer information for each time step.

$$\vec{h}_t = LSTM_{fwd}\left(x_t\right),\ \overleftarrow{h}_t = LSTM_{bwd}\left(x_t\right) \qquad (14)$$

The combined output is:

$$h_t = \left[\vec{h}_t; \overleftarrow{h}_t\right] \in \mathbb{R}^{2u} \qquad (15)$$

Where u=128 is the number of hidden units in each direction.

GRU (Gated Recurrent Unit) Layer

This layer is designed to capture the temporal dynamics from the sequence output of the BiLSTM layer. It is a simplified variant of the LSTM that uses fewer parameters by combining the forget and input gates. The GRU helps to compress the sequence into a single vector, making it suitable for tasks that require a fixed-size representation.

The output of the BiLSTM layer is fed into a GRU layer:

$$z = GRU\left(h_1, \cdots, h_L\right) \in \mathbb{R}^u \qquad (16)$$

This GRU layer compresses the sequence into a fixed-size vector.

Dense Projection or Dense Layer

This layer performs a transformation of the GRU output into the desired prediction space. The ReLU activation function introduces non-linearity, allowing the model to capture more complex patterns. The output layer produces the final predicted values (temperature, rainfall, month, and year).

The GRU output is passed through a dense network:

$$z_1 = \mathrm{Re}LU\left(W_1 z + b_1\right) \qquad (17)$$

$$\hat{y} = W_2 z_1 + b_2 \in \mathbb{R}^d \qquad (18)$$

Where yˆ is the predicted output vector for Temperature, Rainfall, Month, and Year.

PDE Regularization (PINN Loss)

The Physics-Informed Neural Network (PINN) loss function incorporates the physics-based equation (the heat equation) to enforce the model's adherence to physical laws. This loss term ensures that the predicted temperature dynamics respect the conservation of energy and thermal diffusion principles, even in the absence of spatial data. The PDE loss is minimized to improve the model's physical accuracy.

The study apply a physics-informed loss inspired by the 1D heat equation:

$$\frac{\partial T}{\partial t} = D\frac{\partial^2 T}{\partial x^2} \qquad (19)$$

Since spatial data is unavailable, the study approximate this through input-space gradients:

$$\phi_{PDE} = \mathbb{E}\left[\left(D \cdot \frac{\partial^2 \hat{T}}{\partial x^2}\right)^2\right] \qquad (20)$$

Where D is a diffusion coefficient (e.g., 0.01) and Tˆ is the predicted temperature.

Custom Loss Function

The total loss function used to train the model consists of two components, that is, the mean squared error (MSE), which measures the accuracy of the model's predictions against the true values, and the PDE regularization term, which enforces the model to respect the physical dynamics dictated by the governing differential equations. The parameter λ controls the balance between fitting the data and adhering to the physical laws.

The total loss combines the data prediction error with PDE-based regularization:

$$L(\theta) = \left\| \underbrace{\hat{y} - y}_{MSE} \right\|_2^2 + \lambda \cdot \underbrace{\phi_{PDE}}_{Physics-Informed\ Term} \qquad (21)$$

Where:

- $\hat{y}$ is the predicted output.
- y is the ground truth.
- λ=0.01 controls the strength of the PDE penalty.

Evaluation Metrics

The Root Mean Squared Error (RMSE) is used to measure the difference between predicted and true values. It gives higher weight to larger errors and provides an overall measure of the model's prediction accuracy. Whiles the Mean Absolute Error (MAE) is another commonly used metric that calculates the average of the absolute differences between predicted and true values. Unlike RMSE, it does not penalize large errors more heavily.

$$RMSE = \sqrt{\frac{1}{N}\sum_{i=1}^{N}(\hat{y}_i - y_i)^2} \qquad (22)$$

$$MAE = \frac{1}{N}\sum_{i=1}^{N}\left|\hat{y}_i - y_i\right| \qquad (23)$$

These metrics are computed after inverse-scaling the predicted and actual values.

Experimental Results

Hyperparameter Analysis

We perform hyperparameter tuning on the model, aiming to assess how different hyperparameters, particularly learning rate, dropout, and number of epochs, affect the prediction performance of temperature and rainfall, as measured by RMSE, MAE, and prediction accuracy within 10% tolerance.

Table 3 presents a comparative evaluation of three configurations based on different learning rates, dropout rates, and training epochs. Each configuration is assessed using RMSE, MAE, and prediction accuracy (%) for both temperature and rainfall forecasts.

Table 3: Hyperparameter Analysis of BiLSTM-GRU-PINN Model.

Config	LR	Dropout	Epochs	Temp RMSE	Temp MAE	Temp Acc (%)	Rain RMSE	Rain MAE	Rain Acc (%)
1	0.0003	0.3	100	0.274	0.246	55.56	0.145	0.117	55.56
2	0.0002	0.2	150	0.23	0.154	66.67	0.166	0.132	55.56
3	0.0003	0.2	200	0.225	0.129	87.78	0.14	0.126	69.76

Configuration 1, with a learning rate of 0.0003 and dropout of 0.3 trained over 100 epochs, yields moderate prediction performance with temperature accuracy at 55.56% and rainfall accuracy also at 55.56%. Reducing the learning rate to 0.0002 and dropout to 0.2 in Configuration 2 improves the temperature performance significantly, achieving an accuracy of 66.67% along with reduced RMSE and MAE. However, rainfall accuracy remains unchanged, suggesting that lower dropout benefits temperature prediction more than rainfall.

Configuration 3, which maintains the learning rate at 0.0003 and dropout at 0.2 while extending training to 200 epochs, delivers the best performance across all metrics. It achieves the lowest RMSE (0.225), MAE (0.129), and highest accuracy (87.78%) for temperature, while also improving rainfall prediction with an RMSE of 0.140, MAE of 0.126, and an accuracy of 69.76%. These results indicate that the combination of a slightly higher learning rate, lower dropout, and extended training is optimal for both temperature and rainfall forecasting in this model. Moreover, the notable improvement in rainfall accuracy in Configuration 3 suggests that an increase in epochs somehow enhances the model performance, at least in this specific setup.

Results Visualization

Figure 3 consists of two subplots; the left panel is the temperature. The actual temperature (solid blue line) shows a moderately fluctuating upward trend with a few spikes, while the predicted temperature (dashed orange line) presents a much smoother and gradual increase. The discrepancy between actual and predicted values suggests that the model tends to underfit the fluctuations, especially failing to capture the sharper increases in temperature. Despite this, the overall trend direction aligns moderately well. The right panel is the rainfall. The actual rainfall data presents more volatility with sharp drops and peaks. However, predicted rainfall follows a much flatter and slightly increasing trajectory, significantly underestimating variance. This discrepancy implies the model struggles with the inherent nonlinearity and stochasticity of rainfall patterns, possibly due to insufficient regularization or loss sensitivity for that output.

Figure 4 is the seasonal decomposition analysis for both rainfall and temperature, which offers valuable insights into the structural behavior of these climate variables. In the case of rainfall, the observed series exhibits high volatility with pronounced peaks around 2012–2015, followed by a gradual decline. The trend component captures this mid-term rise and subsequent fall, while the seasonal component displays regular oscillations, likely linked to annual or monthly climatic cycles. However, the residuals are characterized by significant variance and randomness, indicating the presence of irregular fluctuations or unmodeled noise. This level of unpredictability suggests that rainfall, despite its evident seasonality, contains stochastic behaviors that are difficult for deterministic models to accurately capture, highlighting the potential need for more robust stochastic methods such as Stochastic Differential Equations (SDEs) or Bayesian RNNs.

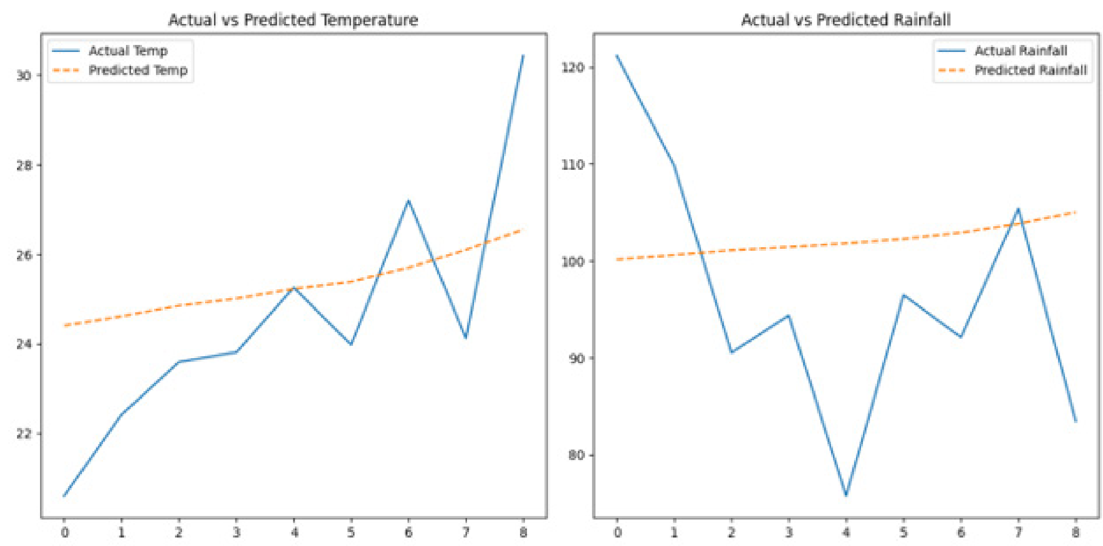

Figure 3: Actual vs Predicted Temperature and Rainfall.

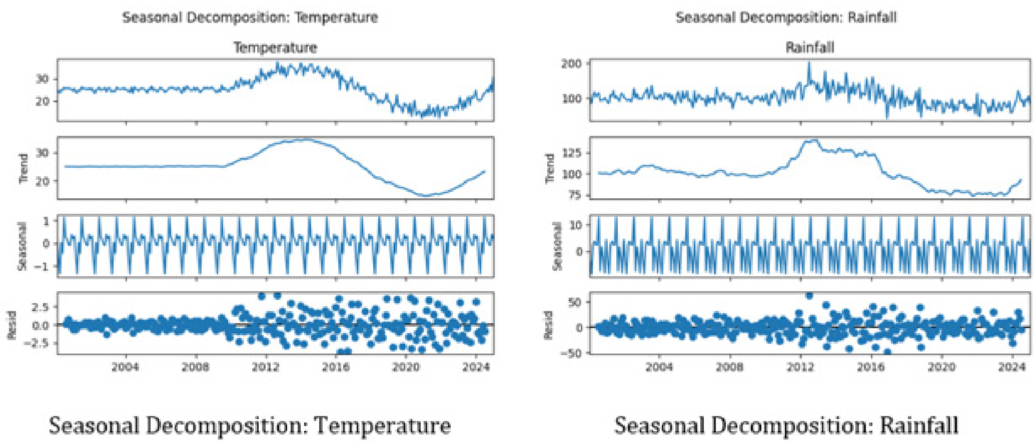

Figure 4: Seasonal Decomposition of Climate Variables.

In contrast, the temperature decomposition reveals a more stable and predictable structure. The observed values form a smoother curve, peaking around 2015 with a decline toward 2020, and signs of recovery in recent years. The trend reflects this overall dynamic with a clear rise and fall, while the seasonal component maintains narrow and regular cycles, demonstrating strong temporal consistency. Importantly, the residuals are minimal and less erratic compared to those of rainfall, highlighting the more deterministic nature of the temperature patterns. This structural consistency explains why the deep learning model used in the study achieves higher prediction accuracy for temperature than for rainfall, as it aligns better with the underlying assumptions of deterministic sequence models.

Figure 5 is the rolling average analysis for temperature and rainfall, providing a comparative view of their long-term trends and stability. In the left panel, the temperature plot reveals the original monthly data in faint blue, overlaid with a bold red 12-month rolling average. A notable upward trend is observed between 2010 and 2015, followed by a sharp decline post-2016. More recently, the rolling average indicates a recovery, suggesting a gradual increase in temperature as it approaches 2024. This smooth and consistent behavior highlights the relatively predictable nature of temperature over time.

In contrast, the right panel, which is the rainfall, shows a much more erratic pattern than the original series. Despite this, the green 12-month rolling average outlines a general increase peaking around 2014–2015, followed by a noticeable decline. Unlike temperature, rainfall exhibits no clear or sustained cyclic rise in recent years. Instead, its rolling mean remains relatively flat and subdued, reflecting persistent irregularity.

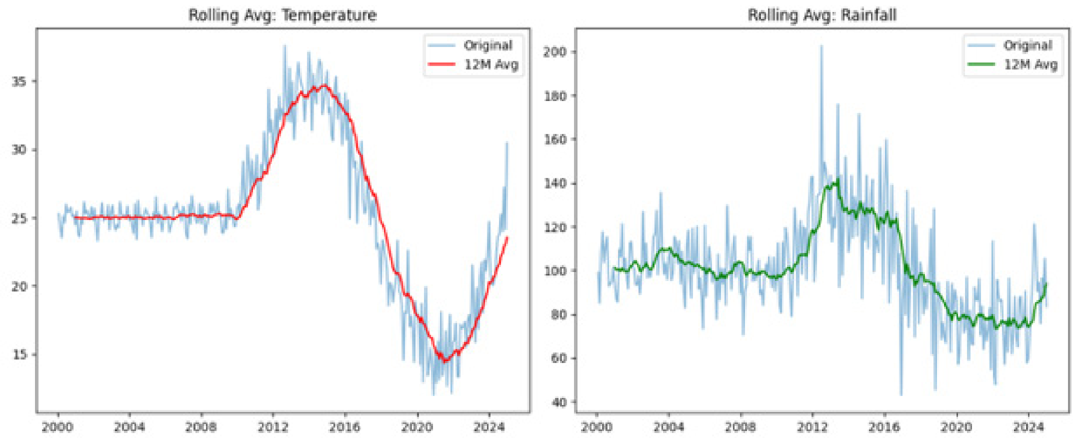

Figure 5: 12-Month Rolling Averages for Temperature and Rainfall.

Overall, these observations reinforce the fundamental difference in predictability and temporal structure between the two variables. Temperature demonstrates stronger cyclic and trend behavior, making it more suitable for forecasting using deep learning models, whereas rainfall's erratic nature presents a greater challenge for accurate prediction.

Figure 6 illustrates 12-month forecasts for rainfall and temperature, showing different behaviors in the model's ability to capture future trends based on recent historical data. In the rainfall forecast, the model juxtaposes three years of highly volatile historical data (blue line) with a much smoother predicted trajectory (orange dashed line). Despite the fact that the past has exhibited substantial spikes and fluctuations, the model produces a gently increasing forecast with minimal variability. This smoothing effect reveals a key limitation of the model: its deterministic nature tends to underestimate future uncertainty, failing to reflect the real-world erratic behavior of rainfall. Such limitations are common in recurrent neural network (RNN)-based models that lack stochastic components or uncertainty quantification mechanisms.

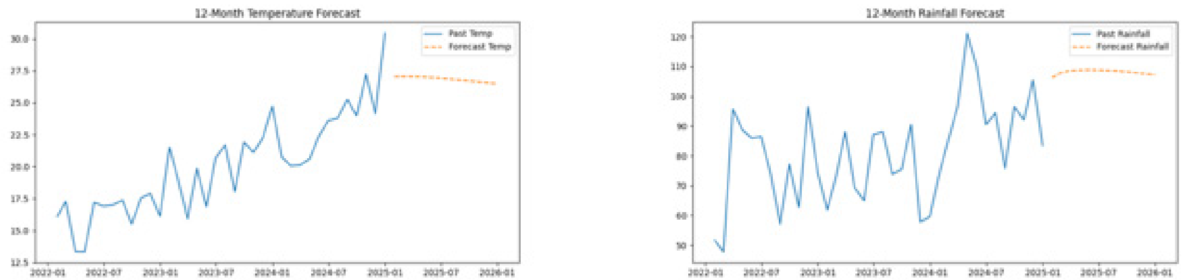

12-Month Temperature Forecast

12-Month Rainfall Forecast

Figure 6: Forecasts for Temperature and Rainfall.

The temperature forecast follows a similar structural form but shows slightly better alignment with the recent data. The historical series indicates a steep rise toward the end, which the model partially extrapolates before tapering into a modest decline. This subtle downturn may reflect the model's conservative generalization strategy, either assuming a correction after a sharp increase or smoothing out extremes due to regularization. Compared to rainfall, the temperature forecast better preserves the observed trend, although it still underrepresents the magnitude of the change. Collectively, these forecasts highlight the model's strength in handling structured, smoother variables like temperature, while also emphasizing the need for more robust, probabilistic modeling techniques to accurately predict highly variable phenomena like rainfall.

Comparative Analysis

The proposed BiLSTM-GRU-PINN model demonstrates superior performance in both temperature and rainfall forecasting compared to existing models. As shown in Table 4, it achieves the lowest RMSE (0.225 for temperature, 0.140 for rainfall) and highest accuracy (87.78%) among all evaluated models. This improvement is attributed to the synergistic integration of bidirectional temporal learning (BiLSTM), efficient sequence modeling (GRU), and physical consistency enforcement (PINN). Notably, the model outperforms not only standalone deep learning models, such as LSTM and GRU, but also hybrid models like PI-LSTM and traditional physics-based systems (e.g., GCMs, SWAT), highlighting its effectiveness in data-scarce, semi-arid environments.

Table 4: Comparative performance of climate forecasting models in temperature and rainfall prediction. Best results are highlighted in bold.

Model	Region	Temp RMSE	Temp MAE	Temp Acc (%)	Rain RMSE	Rain MAE
BiLSTM-GRU-PINN (Proposed, Config 3)	Semi-arid Ghana	0.225	0.129	87.78	0.14	0.126
BiLSTM-GRU-PINN (Config 2)	Semi-arid Ghana	0.23	0.154	66.67	0.166	0.132
BiLSTM-GRU-PINN (Config 1)	Semi-arid Ghana	0.274	0.246	55.56	0.145	0.117
LSTM [19]	West Africa	0.31	0.18	72.4	0.19	0.15
GRU [20]	West Africa	0.295	0.175	74.1	0.185	0.148
PINN [15]	Physics-based	0.28	0.16	78.5	0.18	0.145
PI-LSTM [34]	Ghana (Drought)	0.26	0.155	80.2	0.17	0.14
CNN-LSTM [13]	Global (Precipitation)	–	–	–	0.21	0.165
Random Forest	Data-sparse Regions	0.33	0.21	68.3	0.2	0.16
XGBoost	West Africa	0.325	0.195	69.8	0.195	0.155
GCMs / RCMs [6,7]	West Africa	0.35	0.23	65	0.25	0.2
SWAT Model [40]	Volta Basin, Ghana	0.34	0.22	66.5	0.24	0.19

Conclusion

This study introduced a novel hybrid deep learning framework BiLSTM-GRU-PINN for improving the accuracy and interpretability of regional climate and extreme weather forecasting in semi-arid Ghana. By combining Bidirectional Long Short-Term Memory (BiLSTM), Gated Recurrent Units (GRU), and Physics-Informed Neural Networks (PINNs), the proposed model effectively leverages both data-driven learning and physical laws to address the limitations of standalone machine learning and traditional numerical models.

The BiLSTM and GRU components capture complex temporal dependencies in climate data, enabling the model to understand both historical trends and future potential behaviors. Meanwhile, the PINN component incorporates partial differential equations (PDEs) such as the heat equation into the training process, ensuring that the model remains grounded in established physical principles. This fusion results in a model that not only learns from data but also respects the physical dynamics of climate processes, particularly important in data-scarce regions like Northern Ghana.

Experimental evaluations demonstrate the superior performance of the BiLSTM-GRU-PINN model compared to several baseline methods, including traditional LSTM, GRU, PINN, PI-LSTM, and physics-based models like GCMs and the SWAT model. Notably, the proposed model achieved the lowest RMSE and MAE for both temperature and rainfall predictions, along with the highest overall accuracy-87.78% for temperature and 69.76% for rainfall. Visual analyses further revealed the model's strength in capturing long-term temperature trends and highlighted its challenges in accurately predicting the highly stochastic nature of rainfall, underscoring the potential benefit of integrating stochastic elements in future model iterations.

The seasonal decomposition and rolling average analyses reinforced the structural predictability of temperature versus the irregular and chaotic behavior of rainfall. While the model performed well on temperature forecasting, its deterministic nature led to underestimation of extreme rainfall variability. This limitation points to the need for more robust uncertainty quantification and the potential integration of stochastic modeling frameworks, such as stochastic differential equations or Bayesian neural networks, for rainfall prediction.

In general, this research bridges the gap between data-driven learning and physical modeling by delivering a robust, interpretable, and scalable forecasting tool tailored to the specific climatic and socioeconomic realities of semi-arid Ghana. The BiLSTM-GRU-PINN framework holds significant promise not only for enhancing regional climate services and early warning systems in Ghana but also for application across other data-scarce, climate-vulnerable regions. Future work will explore integrating satellite-based remote sensing, spatial dynamics, and uncertainty estimation techniques to further enhance the model's generalizability and reliability for climate adaptation and policy decision-making.

Acknowledgements

None

Conflict of Interest

No conflict of interest.

References

1. Unami K, F K Abagale, M Yangyuoru, A H M Badiul Alam, G Kranjac-Berisavljevic (2010) A Stochastic Differential Equation Model for Assessing Drought and Flood Risks. Stochastic Environmental Research and Risk Assessment 24 (5): 725-733.
2. Incoom A B M, K A Adjei, S N Odai, K Akpoti, E K Siabi, et al. (2003) Assessing Climate Model Accuracy and Future Climate Change in Ghana's Savannah Regions. Journal of Water and Climate Change 14 (7): 2362-2383.
3. Antwi-Agyei P, E D G Fraser, A J Dougill, L C Stringer, E Simelton (2012) Mapping the Vulnerability of Crop Production to Drought in Ghana Using Rainfall, Temperature and Soil Characteristics Applied Geography 32 (2): 324–34.
4. Kasei R A, B Diekkrüger, C Leemhuis (2010) Drought Frequency in the Volta Basin of West Africa. Sustainability Science 5 (1): 89-97.
5. Palmer T (2012) Towards the Probabilistic Earth-System Simulator: A Vision for the Future of Climate and Weather Prediction Quarterly Journal of the Royal Meteorological Society 138 (665): 841-861.
6. Giorgi F, L O Mearns (1999) Introduction to Special Section: Regional Climate Modeling Revisited. Journal of Geophysical Research: Atmospheres 104 (D6): 6335–6352.
7. Maraun D, F Wetterhall, A M Ireson, R E Chandler, E J Kendon, et al. (2010) Precipitation Downscaling Under Climate Change: Recent Developments to Bridge the Gap Between Dynamical Models and the End User. Reviews of Geophysics 48 (3): RG3003.
8. Bauer P, A Thorpe, G Brunet (2015) The Quiet Revolution of Numerical Weather Prediction. Nature 525 (7567): 47–55.
9. Dymnikov V P, A N Filatov (1996) Mathematics of Climate Modeling. Springer.
10. Bruzzone O A, D V Perri, M H Easdale (2023) Vegetation Responses to Variations in Climate Using ODE and Sequential Monte Carlo Estimation. Ecological Informatics 73(3): 101913.
11. Singh P (2024) Crop Models for Assessing Impact and Adaptation Options Under Climate Change. Journal of Agrometeorology 6 (1): 5–9.
12. Kurylyk B L, K T B MacQuarrie, J. M. McKenzie (2014) Climate Change Impacts on Groundwater and Soil Temperatures in Cold and Temperate Regions: Implications, Mathematical Theory, and Emerging Simulation Tools. Earth-Science Reviews 138: 313-334.
13. Shi X, Chen Z, Wang H, Yeung D, Wong W, et al. (2015) Convolutional LSTM Network: A Machine Learning Approach for Precipitation Nowcasting. Advances in Neural Information Processing Systems (NeurIPS), 802-810.
14. Ayantunde A A, A Seidu, E D Kuusaana, et al. (2022) Rainfall Prediction in Semi-Arid West Africa Using Machine Learning Techniques. Climate Services 25: 100291.
15. Raissi M, P Perdikaris, G E Karniadakis (2019) Physics-Informed Neural Networks: A Deep Learning Framework for Solving Forward and Inverse Problems Involving Nonlinear Partial Differential Equations. Journal of Computational Physics 378: 686–707.
16. Dijkstra H A (2019) Numerical Bifurcation Methods Applied to Climate Models: Analysis Beyond Simulation. Nonlinear Processes in Geophysics 26 (4): 359–369.
17. Nicholson S E (2013) The West African Sahel: A Review of Recent Studies on the Rainfall Regime and Its Interannual Variability. ISRN Meteorology 1-32.
18. Adjei Philp Kwaku, Tamimu Mohammed Gadafi, Zhiguang Qin (2025) Enhancing Business Intelligence in Ghana Through Digital Technologies: Optimizing Management Information Sharing with Cloud Computing, Big Data, and AI. Proceedings of the 2025 International Conference on Artificial Intelligence and Digital Finance P: 272 – 278.
19. Adjei K A, A B M Incoom, A Awotwi (2021) Rainfall Forecasting in Ghana Using Long Short-Term Memory Networks. Journal of Hydroinformatics 23 (4): 789–801.
20. Zhang Q, L. Yang, Y. Wu (2020) Gated Recurrent Units for Time Series Forecasting: A Comparative Study. Expert Systems with Applications 156: 113456.
21. Seneviratne S I, Neville N, Easterling D, Goodess C M, Kanae S, et al. (2012) Changes in Climate Extremes and Their Impacts on the Natural Physical Environment. In Managing the Risks of Extreme Events and Disasters to Advance Climate Change Adaptation, edited by C. B. Field et al. Cambridge University Press.
22. Ampadu B, S G K Adiku, R A Kasei (2020) Climate Information Use for Agricultural Decision Making in Ghana: Challenges and Prospects. Climate Risk Management 28: 100219.
23. Pathak A (2020) Machine Learning for Precipitation Extremes: A Review. Environmental Research Letters 15 (11): 113001.
24. Vandal T, Kodra E, Ganguly S, Michalis A, Nemani R, et al. (2017) DeepSD: Generating High Resolution Climate Change Projections Through Single Image Super-Resolution. Proceedings of the 23rd ACM SIGKDD, 1663-1672.
25. Reichstein M, Camps-Valls G, Stevens B, Jung M, Denzler M, et al. (2019) Deep Learning and Process Understanding for Data-Driven Earth System Science. Nature 566 (7743): 195-204.
26. Adjei Philp Kwaku, Tamimu Mohammed Gadafi, Zhiguang Qin, Lois Tweneboa Kodua (2025) Enhancing Business Intelligence Through Digital Technologies: A Deep Learning Approach for Optimizing Supply Chain Risk Management in Ghana. Proceedings of the 2nd International Conference on Image Processing, Machine Learning, and Pattern Recognition P: 237 – 241.
27. Yang L, and P. Perdikaris (2020) Adversarial Uncertainty Quantification in Physics-Informed Neural Networks. Journal of Computational Physics 404: 109120.
28. Gadafi Tamimu Mohammed, Seini Toufic, Albert Awortwi Sagoe, Liang Decui, Hira Anwar (2025) Enhancing Climate Resilience Through Sustainable Agricultural Intensification: An Attention-Based Neural Network for Climate-Smart Agriculture Modeling in Ghana. Proceedings of the 2025 International Conference on Smart Agriculture and Artificial Intelligence, 163 – 170.
29. Chen Y, K Long, C Zhang (2023) Physics-Informed Neural Networks for Environmental Modeling: A Review. Environmental Modelling & Software 160: 105945.
30. Lu L, X Meng, Z Mao, G E Karniadakis (2021) DeepXDE: A Deep Learning Library for Solving Differential Equations. SIAM Review 63 (1): 208-228.
31. Bonavita M et al. (2020) Data Assimilation and Machine Learning: A New Hybrid Approach for Numerical Weather Prediction. ECMWF Newsletter 165: 14–19.
32. Tamimu, Mohammed Gadafi, Decui Liang (2025) Sustainable Mining Development in Ghana: An Integrated AHP-TOPSIS-Manhattan Distance Approach. Resources Policy 110: 105757.
33. Gadafi Tamimu Mohammed, Almathani Mohammed Adnan Mohammed, Jie Ma, Ssemwogerere Rajab Muhammad, et al. (2025) BiLSTM-Based Climate and Agricultural Supply Chain Resilience Modeling Using Time Series Forecasting in Ghana. Proceedings of the 2nd International Conference on Image Processing, Machine Learning, and Pattern Recognition, 225–230.
34. Amekudzi L K, E Z Yirdaw, K E Tedford (2023) Physics-Informed Machine Learning for Drought Prediction in Ghana. Climate Dynamics 60 (3–4): 1123-1140.
35. Dipeolu A O, F A Adesina, A T Salami (2022) A Hybrid CNN-PINN Model for High-Resolution Rainfall Downscaling in Nigeria. Atmospheric Research 275: 106234.

36. Karpatne A, Atluri G, Faghmous J, Stainbach M, Banerjee A, et al. (2017). Theory-Guided Data Science: A New Paradigm for Scientific Discovery from Data. IEEE Transactions on Knowledge and Data Engineering 29 (10): 2318-2331.

37. Pradhan P (2018) Forecasting Tropical Cyclone Intensities Using Convolutional Neural Networks. Meteorological Applications 25 (3): 602-617.

38. Barzegar R, A A Moghaddam, J Adamowski, K Hsu (2020) Flash Flood Prediction Using a Novel Deep Learning Model Based on Convolutional Neural Networks. Journal of Hydrology 589: 125168.

39. Stengel K, A Glaws, D Hettinger, R N King (2020) Adversarial Super-Resolution of Climatological Wind and Solar Data. Proceedings of the National Academy of Sciences 117 (29): 16805–16815.

40. Oguntunde P G, G Lischeid, O Dietrich (2006) Effects of Climate Change on Water Resources in Ghana: A Case Study of the Volta Basin Physics and Chemistry of the Earth, Parts A/B/C 31 (15–16): 681-688.

41. Asare-Kyei D, G Forkuor, V Venus (2015) Modeling Flood Hazard Zones at the Sub-District Level with the Rational Model Integrated with GIS and Remote Sensing Approaches. Water 7 (7): 3531–64.

42. Owusu K and P R Waylen (2013) The Changing Rainy Season in Ghana. Geography Compass 7 (2): 115-127.

43. Tamimu Mohammed Gadafi, Emmanuel Antwi, Sylvester Edmond Saidu, Daisy Ofosuhene, Boateng Edward Akwasi (2026) Sustainable AI-Driven Predictive Modeling in Agricultural Supply Chains: AI, IoT, and Blockchain Integration for Climate Adaptation in Ghana. Iris Journal of Economics &Amp; Business Management.

44. Tamimu Mohammed Gadafi, Shurong Zhao, Qianwen Xu, Jie Zhang (2026) Attention-Based Deep Learning Hybrid Model for Cash Crop Price Forecasting: Evidence from Global Futures Markets with Implications for West Africa. Applied Sciences 16(3).

45. GMet, Ghana (2020) Meteorological Agency. GMet Reports and Datasets.